

Pseudoscalar Decay Constants f_D and f_{D_s} in Lattice QCD with Exact Chiral Symmetry

Ting-Wai Chiu, Tung-Han Hsieh, Jon-Yu Lee, Pei-Hua Liu, Hsiu-Ju Chang

Department of Physics and
National Center for Theoretical Sciences at Taipei,
National Taiwan University, Taipei 106, Taiwan

Abstract

We determine the masses and decay constants of pseudoscalar mesons D , D_s , and K in quenched lattice QCD with exact chiral symmetry. For 100 gauge configurations generated with single-plaquette action at $\beta = 6.1$ on the $20^3 \times 40$ lattice, we compute point-to-point quark propagators for 30 quark masses in the range $0.03 \leq m_q a \leq 0.80$, and measure the time-correlation functions of pseudoscalar and vector mesons. The inverse lattice spacing a^{-1} is determined with the experimental input of f_π , while the strange quark bare mass $m_s a = 0.08$, and the charm quark bare mass $m_c a = 0.80$ are fixed such that the masses of the corresponding vector mesons are in good agreement with $\phi(1020)$ and $J/\psi(3097)$ respectively. Our results of pseudoscalar-meson decay constants are $f_K = 152(6)(10)$ MeV, $f_D = 235(8)(14)$ MeV, and $f_{D_s} = 266(10)(18)$ MeV.

PACS numbers: 11.15.Ha, 11.30.Rd, 12.38.Gc

Keywords: Lattice QCD, Exact Chiral Symmetry, Pseudoscalar-Meson Decay Constant

1 Introduction

The pseudoscalar-meson decay constants (e.g., f_D , f_{D_s} , f_B and f_{B_s}) play an important role in extracting the CKM matrix elements (e.g., the leptonic decay width of $D_s^+ \rightarrow l^+ \nu_l$ is proportional to $f_{D_s}^2 |V_{cs}|^2$), which are crucial for testing the flavor sector of the standard model via the unitarity of CKM matrix. Experimentally¹, precise determination of f_{D_s} and f_D will soon result from the high-statistics program of CLEO-c, however, the determination of f_B and f_{B_s} remains beyond the reach of current experiments.

Theoretically, lattice QCD provides a solid framework to compute the masses and decay constants of pseudoscalar mesons (as well as other physical observables) nonperturbatively from the first principles of QCD. Thus reliable lattice QCD determinations of f_B and f_{B_s} are of fundamental importance, in view of their experimental determinations are still lacking. Obviously, the first step for lattice QCD is to check whether the lattice determinations of f_D and f_{D_s} will agree with those coming soon from the high-statistics charm program of CLEO-c. This motivates our present study.

In this paper, we compute quenched quark propagators for 30 quark masses in the range $0.03 \leq m_q a \leq 0.80$, in the framework of optimal domain-wall fermion proposed by Chiu [10]-[12]. Then we determine the inverse lattice spacing $a^{-1} = 2.237(76)$ GeV from the pion time-correlation function, with the experimental input of pion decay constant $f_\pi = 132$ MeV. The strange quark bare mass $m_s a = 0.08$ and the charm quark bare mass $m_c a = 0.80$ are fixed such that the corresponding masses extracted from the vector meson correlation function agree with $\phi(1020)$ and $J/\psi(3097)$ respectively. Then the masses and decay constants of any hadrons containing c , s , and $u(d)$ quarks² are predictions of QCD from the first principles, with the understanding that chiral extrapolation to physical $m_{u,d} \simeq m_s/25$ (or equivalently $m_\pi = 135$ MeV) is required for any observables containing $u(d)$ quarks.

For pseudoscalar and vector mesons, we measure their time correlation functions for the following three categories: (i) two quarks have the same mass; (ii) one quark mass is fixed at m_s ; (iii) one quark mass is fixed at m_c . Note that for mesons which are composed of strange and/or charm quarks, their masses and decay constants can be measured directly without chiral extrapolation.

The outline of this paper is as follows. In section 2, we outline our formulation of exact chiral symmetry on the lattice, and our computation of quark propagators. In section 3, we determine the inverse lattice spacing, the strange quark bare mass, and the charm quark bare mass. In section 4, we present our results of m_K and f_K . In section 5, we present our results of m_D , m_{D_s} , f_D , and f_{D_s} . In section 6, we summarize our results and conclude with some remarks.

¹See, for example, Refs. [1, 2, 3, 4], and other experimental results compiled by PDG [5].

²In this paper, we work in the isospin limit $m_u = m_d$.

2 Lattice quarks with exact chiral symmetry

To implement exact chiral symmetry on the lattice [6, 7, 8, 9], we consider the optimal domain-wall fermion proposed by Chiu [10]-[12]. The action of optimal domain-wall fermion can be written as [12]

$$\begin{aligned} \mathcal{A}_F = \sum_{s,s'=0}^{N_s+1} \sum_{x,x'} \bar{\psi}(x,s) \{ & (\omega_s D_w(x,x') + \delta_{x,x'}) \delta_{ss'} \\ & + (\omega_s D_w(x,x') - \delta_{x,x'}) (P_+ \delta_{s',s-1} + P_- \delta_{s',s+1}) \} \psi(x',s') \end{aligned} \quad (1)$$

with boundary conditions

$$\begin{aligned} P_+ \psi(x, -1) &= -r m_q P_+ \psi(x, N_s + 1), \\ P_- \psi(x, N_s + 2) &= -r m_q P_- \psi(x, 0), \quad r = \frac{1}{2m_0}, \end{aligned}$$

where m_q is the bare quark mass, and $\{\omega_s, s = 0, \dots, N_s + 1\}$ are specified by the exact formula derived in Ref. [10]. Here $H_w = \gamma_5 D_w$, and D_w is the standard Wilson Dirac operator plus a negative parameter $-m_0$ ($0 < m_0 < 2$). The quark fields are constructed from the boundary modes at $s = 0$ and $s = N_s + 1$ with $\omega_0 = \omega_{N_s+1} = 0$ [12]:

$$q(x) = \sqrt{r} [P_- \psi(x, 0) + P_+ \psi(x, N_s + 1)], \quad (2)$$

$$\bar{q}(x) = \sqrt{r} [\bar{\psi}(x, 0) P_+ + \bar{\psi}(x, N_s + 1) P_-]. \quad (3)$$

After introducing pseudofermions with $m_q = 2m_0$, the generating functional for n -point Green's function of the quark fields can be derived as [12],

$$Z[J, \bar{J}] = \frac{\int [dU] e^{-\mathcal{A}_g} \det[(D_c + m_q)(1 + rD_c)^{-1}] \exp \left\{ \bar{J} (D_c + m_q)^{-1} J \right\}}{\int [dU] e^{-\mathcal{A}_g} \det[(D_c + m_q)(1 + rD_c)^{-1}]} \quad (4)$$

where \mathcal{A}_g is the action of the gauge fields, \bar{J} and J are the Grassman sources of q and \bar{q} respectively, and

$$D_c = 2m_0 \frac{1 + \gamma_5 S_{opt}}{1 - \gamma_5 S_{opt}}, \quad (5)$$

$$S_{opt} = \frac{1 - \prod_{s=1}^{N_s} T_s}{1 + \prod_{s=1}^{N_s} T_s}, \quad (6)$$

$$T_s = \frac{1 - \omega_s H_w}{1 + \omega_s H_w}. \quad (7)$$

Using the exact formula of ω_s [10], one immediately obtains

$$S_{opt} = \begin{cases} H_w R_Z^{(n,n)}(H_w^2), & N_s = 2n + 1, \\ H_w R_Z^{(n-1,n)}(H_w^2), & N_s = 2n, \end{cases} \quad (8)$$

where $R_Z(H_w^2)$ is the Zolotarev optimal rational polynomial [13] for the inverse square root of H_w^2 ,

$$\begin{aligned} R_Z^{(n,n)}(H_w^2) &= \frac{d_0}{\lambda_{min}} \prod_{l=1}^n \frac{1 + h_w^2/c_{2l}}{1 + h_w^2/c_{2l-1}} \\ &= \frac{1}{\lambda_{min}} (h_w^2 + c_{2n}) \sum_{l=1}^n \frac{b_l}{h_w^2 + c_{2l-1}}, \quad h_w^2 = H_w^2/\lambda_{min}^2 \end{aligned} \quad (9)$$

and

$$R_Z^{(n-1,n)}(H_w^2) = \frac{d'_0}{\lambda_{min}} \frac{\prod_{l=1}^{n-1} (1 + h_w^2/c'_{2l})}{\prod_{l=1}^n (1 + h_w^2/c'_{2l-1})} = \frac{1}{\lambda_{min}} \sum_{l=1}^n \frac{b'_l}{h_w^2 + c'_{2l-1}}, \quad (10)$$

where the coefficients d_0 , d'_0 , c_l and c'_l are expressed in terms of elliptic functions [13] with arguments depending on N_s and $\lambda_{max}^2/\lambda_{min}^2$, and λ_{min} (λ_{max}) is fixed to be the greatest lower bound (least upper bound) of the eigenvalues of $|H_w|$ for the set of gauge configurations under investigation.

From (4), the effective 4D lattice Dirac operator for the fermion determinant is

$$D(m_q) = (D_c + m_q)(1 + rD_c)^{-1} = m_q + (m_0 - m_q/2) \left[1 + \gamma_5 H_w R_Z(H_w^2) \right] \quad (11)$$

and the quark propagator in background gauge field is

$$\begin{aligned} \langle q(x)\bar{q}(y) \rangle &= - \frac{\delta^2 Z[J, \bar{J}]}{\delta \bar{J}(x) \delta J(y)} \Big|_{J=\bar{J}=0} \\ &= (D_c + m_q)_{x,y}^{-1} = (1 - r m_q)^{-1} [D_{x,y}^{-1}(m_q) - r \delta_{x,y}] \end{aligned} \quad (12)$$

Note that D_c is exactly chirally symmetric (i.e. $D_c \gamma_5 + \gamma_5 D_c = 0$) in the limit $N_s \rightarrow \infty$, and its deviation from exact chiral symmetry due to finite N_s is the *minimal* provided that the weights $\{\omega_s\}$ are fixed according to the formula derived in Ref. [10]. Further, the bare quark mass m_q (whether heavy or light) in the quark propagator $(D_c + m_q)^{-1}$ is well-defined for any gauge configurations.

In practice, we have two ways to evaluate the quark propagator (12) in background gauge field:

- (i) To solve the linear system of the 5D optimal DWF operator;
- (ii) To solve $D_{x,y}^{-1}(m_q)$ from the system

$$D(m_q)Y = \left[m_q + (m_0 - m_q/2) \left(1 + \gamma_5 H_w R_Z(H_w^2) \right) \right] Y = \mathbb{1}, \quad (13)$$

with nested conjugate gradient [14], and then substitute the solution vector Y into (12).

Since either (i) or (ii) yields exactly the same quark propagator, in principle, it does *not* matter which linear system one actually solves. However, in

practice, one should choose the most efficient scheme for one's computational system (hardware and software). For our present system (a Linux PC cluster of 100 nodes [15]), it has been geared to the scheme (ii), and it attains the maximum efficiency if the inner conjugate gradient loop of (13) is iterated with Neuberger's 2-pass algorithm [16]. So we use the scheme (ii) to compute the quark propagator, with the quark fields (2)-(3) defined by the boundary modes at $s = 0$ and $s = N_s + 1$. Note that Neuberger's 2-pass algorithm not only provides very high precision of chiral symmetry with fixed amount of memory, but also is faster than the single pass algorithm for $n > 12 \sim 25$ (where n is the order of the rational polynomial $R^{(n-1,n)}$) for most computer platforms, as discussed by Chiu and Hsieh [17].

We generate 100 gauge configurations with single plaquette gauge action at $\beta = 6.1$ on the $20^3 \times 40$ lattice. Fixing $m_0 = 1.3$, we project out 16 low-lying eigenmodes of $|H_w|$ and perform the nested conjugate gradient in the complement of the vector space spanned by these eigenmodes. For $N_s = 128$, the weights $\{\omega_s\}$ are fixed with $\lambda_{min} = 0.18$ and $\lambda_{max} = 6.3$, where $\lambda_{min} \leq \lambda(|H_w|) \leq \lambda_{max}$ for all gauge configurations. For each configuration, point to point quark propagators are computed for 30 bare quark masses in the range $0.03 \leq m_q a \leq 0.8$, with stopping criteria 10^{-11} and 2×10^{-12} for the outer and inner conjugate gradient loops respectively. Then the norm of the residual vector of each column of the quark propagator is less than 2×10^{-11}

$$\|(D_c + m_q)Y - \mathbf{1}\| < 2 \times 10^{-11},$$

and the chiral symmetry breaking due to finite N_s is less than 10^{-14} ,

$$\sigma = \left| \frac{Y^\dagger S^2 Y}{Y^\dagger Y} - 1 \right| < 10^{-14},$$

for every iteration of the nested conjugate gradient. Further details of our scheme have been described in Refs. [18, 17].

In this paper, we measure the time-correlation functions for pseudoscalar (PS) and vector (V) mesons,

$$C_{PS}(t) = \left\langle \sum_{\vec{x}} \text{tr} \{ \gamma_5 (D_c + m_Q)_{x,0}^{-1} \gamma_5 (D_c + m_Q)_{0,x}^{-1} \} \right\rangle_U \quad (14)$$

$$C_V(t) = \left\langle \frac{1}{3} \sum_{\mu=1}^3 \sum_{\vec{x}} \text{tr} \{ \gamma_\mu (D_c + m_Q)_{x,0}^{-1} \gamma_\mu (D_c + m_Q)_{0,x}^{-1} \} \right\rangle_U \quad (15)$$

where the subscript U denotes averaging over gauge configurations. Here $C_{PS}(t)$ and $C_V(t)$ are measured for the following three categories:

- (i) Symmetric masses $m_Q = m_q$,
- (ii) Asymmetric masses with fixed $m_Q = m_s = 0.08a^{-1}$,
- (iii) Asymmetric masses with fixed $m_Q = m_c = 0.80a^{-1}$,

where m_q is varied for 30 masses in the range $0.03 \leq m_q a \leq 0.80$.

3 Determination of a^{-1} , m_s , and m_c

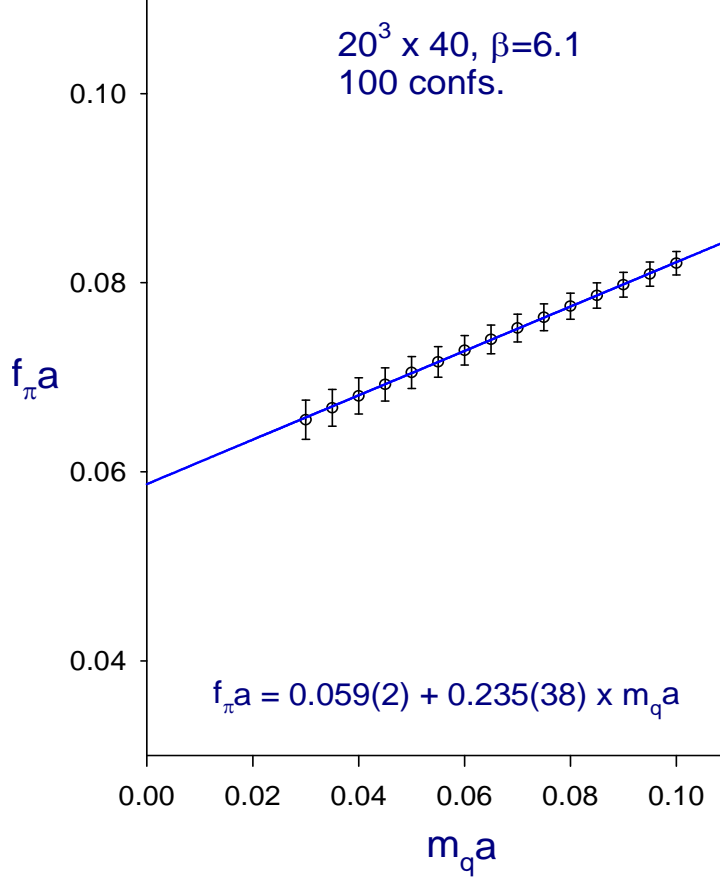


Figure 1: The pion decay constant $f_\pi a$ versus the bare quark mass $m_q a$. The solid line is the linear fit.

For symmetric masses $m_Q = m_q$, the pseudoscalar time-correlation function $C_\pi(t)$ (14) is measured, and is fitted to the usual formula

$$\frac{Z}{2m_\pi a} [e^{-m_\pi a t} + e^{-m_\pi a (T-t)}] \quad (16)$$

to extract the pion mass $m_\pi a$ and the pion decay constant

$$f_\pi a = 2m_q a \frac{\sqrt{Z}}{m_\pi^2 a^2} . \quad (17)$$

In Figs. 1 and 2, we plot the decay constant $f_\pi a$ and pion mass square $(m_\pi a)^2$ versus bare quark mass $m_q a$, respectively.

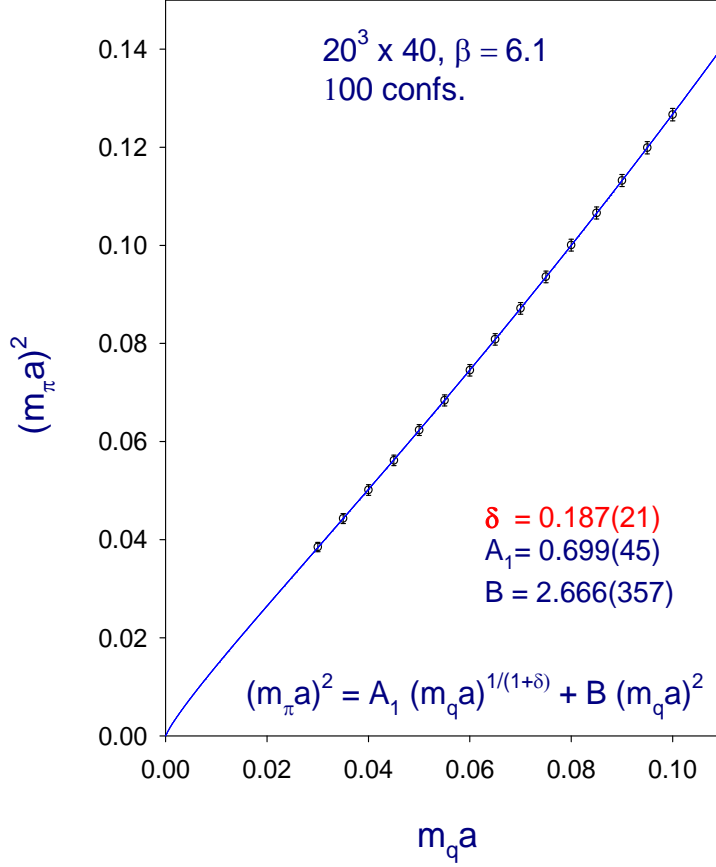


Figure 2: The pion mass square $(m_\pi a)^2$ versus the bare quark mass $m_q a$. The solid line is the fit of Eq. (19).

The data of $f_\pi a$ (see Fig. 1) is well fitted by the straight line

$$f_\pi a = 0.059(2) + 0.235(38) \times (m_q a) .$$

Then taking $f_\pi a$ at $m_q a = 0$ equal to 0.132 GeV times the lattice spacing a , we can determine the lattice spacing a and its inverse,

$$\begin{aligned} a^{-1} &= \frac{0.132}{f_0} \text{ GeV} = 2.237(76) \text{ GeV} , \\ a &= 0.088(3) \text{ fm} . \end{aligned} \tag{18}$$

Thus the size of our lattice is about $(1.8 \text{ fm})^3 \times 3.6 \text{ fm}$. Since the smallest pion mass is 439 MeV, the lattice size is about $(3.9)^3 \times 7.8$, in units of the Compton wavelength ($\sim 0.45 \text{ fm}$) of the smallest pion mass.

The data of m_π^2 (see Fig. 2) can be fitted by the form [19]

$$m_\pi^2 a^2 = A_1 (m_q a)^{\frac{1}{1+\delta}} + B (m_q a)^2 \tag{19}$$

in quenched chiral perturbation theory (q χ PT). The fitted parameters are

$$\delta = 0.187(21) \quad (20)$$

$$A_1 = 0.669(45) \quad (21)$$

$$B = 2.666(357) \quad (22)$$

with $\chi^2/\text{d.o.f.}=0.54$. Evidently, the coefficient of quenched chiral logarithm $\delta = 0.187(21)$ is in good agreement with the theoretical estimate $\delta \simeq 0.176$ in q χ PT.

The bare mass of strange quark is determined by extracting the mass of vector meson from the time-correlation function $C_V(t)$. At $m_q a = 0.08$, $m_V a = 0.460(4)$, which gives $m_V = 1029(10)$ MeV, in good agreement with the mass of $\phi(1020)$. Thus we take the strange quark bare mass to be $m_s a = 0.08$. Similarly, at $m_q a = 0.80$, $m_V a = 1.368(2)$, which gives $m_V = 3060(5)$ MeV, in good agreement with the mass of $J/\Psi(3097)$. Thus, we fix the charm quark bare mass to be $m_c a = 0.80$.

4 f_K and m_K

Next we measure the time-correlation function of kaon $C_K(t)$ (14) with m_Q fixed at $m_s = 0.08a^{-1}$, while m_q is varied for 30 masses in the range $0.03 \leq m_q a \leq 0.80$. Then the data of $C_K(t)$ is fitted by the formula analogous to (16) to extract the kaon mass $m_K a$ and the kaon decay constant $f_K a$.

In Fig. 3, the kaon mass m_K is plotted versus m_π , for 15 quark masses in the range $0.03 \leq m_q a \leq 0.10$. The data of $m_K a$ can be fitted by

$$m_K a = 0.197(1) + 0.255(4)(m_\pi a) + 0.389(8)(m_\pi a)^2 .$$

At the physical limit $m_\pi = 135$ MeV, it gives $m_K = 478(16)$ MeV, in good agreement with the experimental value of kaon mass (495 MeV).

In Fig. 4, $f_K a$ is plotted versus bare quark mass $m_q a$. The data is well fitted by the straight line

$$f_K a = 0.068(0) + 0.116(1) \times (m_q a)$$

At $m_q a = 0$, it gives $f_K = 152(6)$ MeV, in agreement with the value $f_{K^+} = 159.8 \pm 1.4 \pm 0.44$ MeV complied by PDG [5].

5 f_D , f_{D_s} , m_D , and m_{D_s}

Now we turn to charmed pseudoscalar mesons. We measure the time-correlation function $C_D(t)$ (14) with m_Q fixed at $m_c = 0.80a^{-1}$, while m_q is varied for 30 different masses in the range $0.03 \leq m_q a \leq 0.80$. Then the data of $C_D(t)$ is

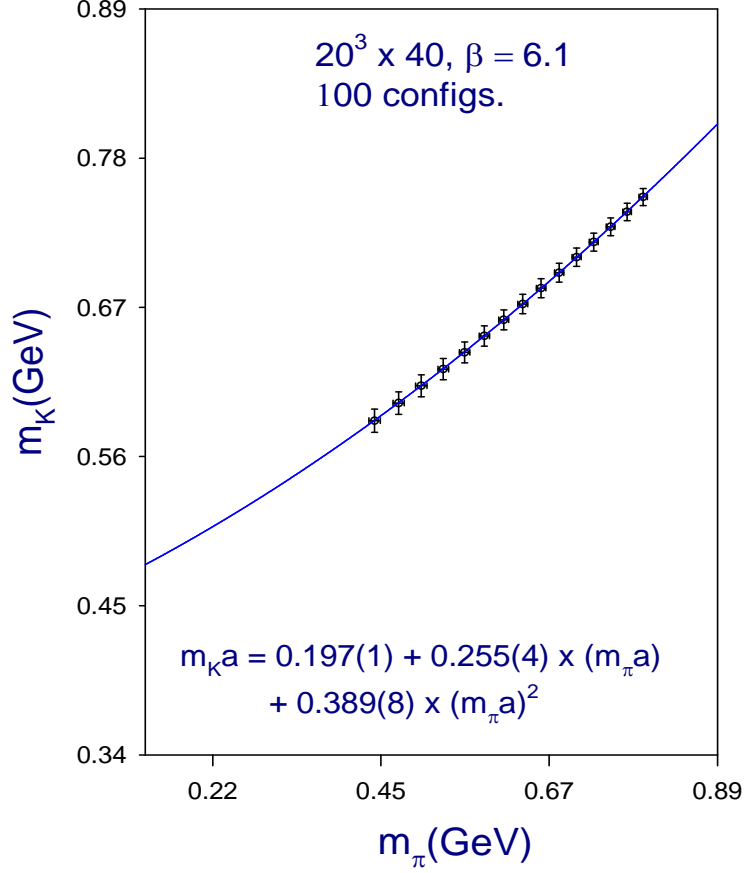


Figure 3: The kaon mass m_K versus the pion mass m_π for 15 bare quark masses in the range $0.03 \leq m_q a \leq 0.10$. The solid line is the quadratic fit.

fitted by the formula analogous to (16) to extract the mass $m_D a$ and decay constant $f_D a$.

In Fig. 5, $m_D a$ is plotted versus $m_\pi a$, for 15 quark masses in the range $0.03 \leq m_q a \leq 0.10$. The data of $m_D a$ can be fitted by

$$m_D a = 0.816(0) + 0.101(3)(m_\pi a) + 0.298(6)(m_\pi a)^2$$

At $m_\pi = 135$ MeV, it gives $m_D = 1842(15)$ MeV, in good agreement with the mass of D meson (1865 MeV). In Fig. 6, the decay constant $f_D a$ is plotted versus bare quark mass $m_q a$. The data is well fitted by the straight line

$$f_D a = 0.105(1) + 0.172(1) \times (m_q a)$$

At $m_q a = 0$, it gives $f_D = 235(8)$ MeV, which serves as a prediction of lattice QCD with exact chiral symmetry.

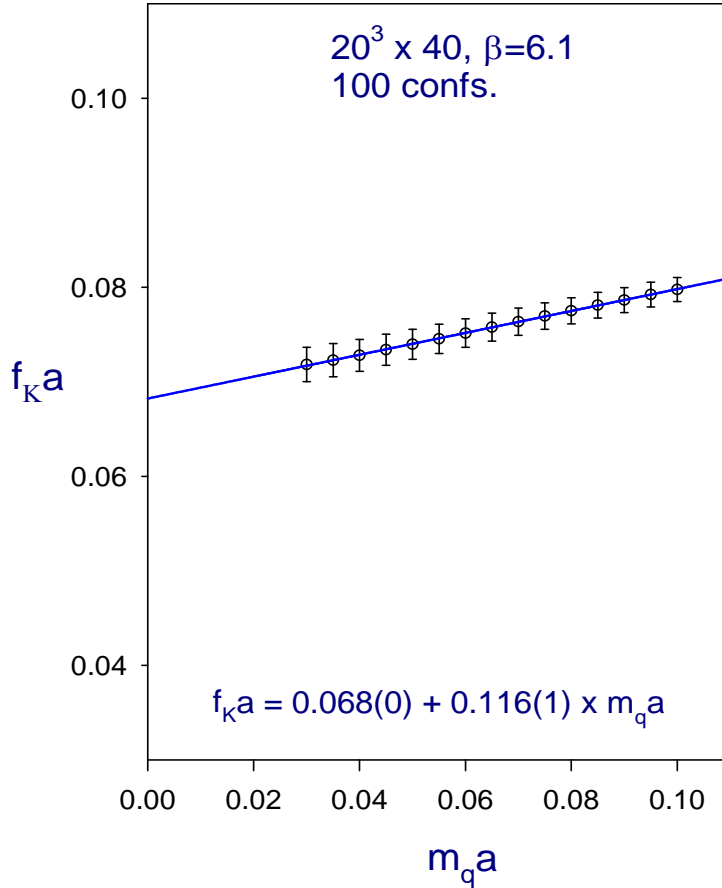


Figure 4: The kaon decay constants $f_K a$ versus the bare quark mass $m_q a$. The solid line is the linear fit.

The pseudoscalar meson of $c\bar{s}$ or $s\bar{c}$ corresponds to $m_Q a = m_c a = 0.80$ and $m_q a = m_s a = 0.08$. Its mass and decay constant are extracted directly from the time-correlation function, which are plotted as the eleventh data point (counting from the smallest one) in Figs. 5 and 6 respectively. The results are $m_{D_s} a = 0.878(2)$ and $f_{D_s} a = 0.119(2)$. The mass gives $m_{D_s} = 1964(5)$ MeV, in good agreement with the mass of $D_s(1968)$. The decay constant gives $f_{D_s} = 266(10)$ MeV, which agrees with the value $f_{D_s^+} = 267 \pm 33$ MeV compiled by PDG [5].

6 Summary and Concluding Remarks

In this paper, we have determined the masses and decay constants of pseudoscalar mesons K , D and D_s , in quenched lattice QCD with exact chiral

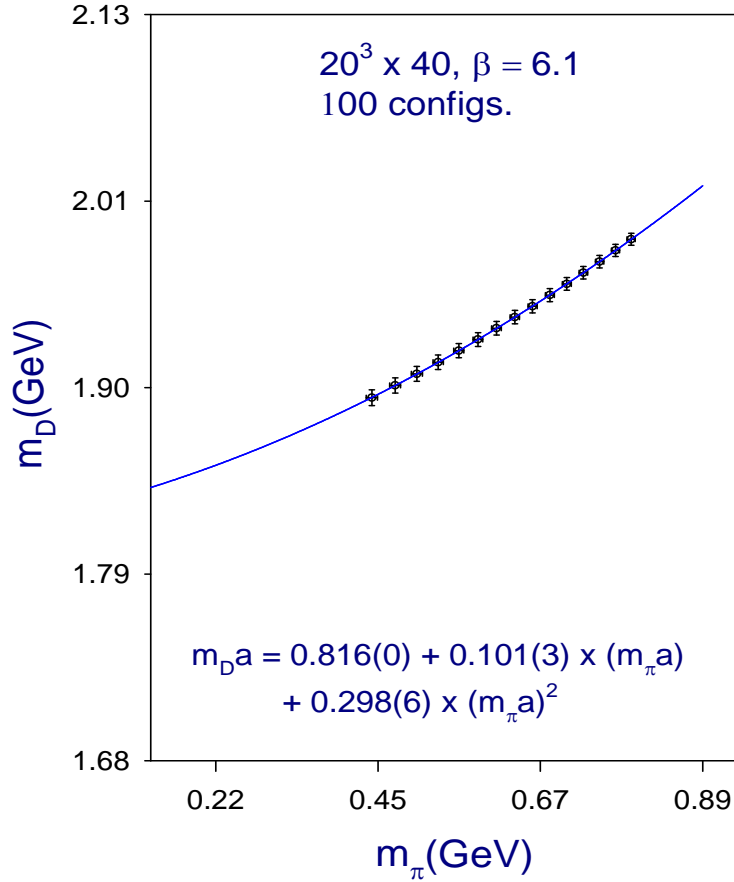


Figure 5: The mass of D meson $m_D a$ versus the pion mass $m_\pi a$ for 15 bare quark masses in the range $0.03 \leq m_q a \leq 0.10$. The solid line is the quadratic fit.

symmetry. Our results are:

$$\begin{aligned}
 m_K &= 478 \pm 16 \pm 20 \text{ MeV}, \\
 m_D &= 1842 \pm 15 \pm 21 \text{ MeV}, \\
 m_{D_s} &= 1964 \pm 5 \pm 10 \text{ MeV}, \\
 f_K &= 152 \pm 6 \pm 10 \text{ MeV}, \\
 f_D &= 235 \pm 8 \pm 14 \text{ MeV}, \\
 f_{D_s} &= 266 \pm 10 \pm 18 \text{ MeV},
 \end{aligned}$$

where in each case, the first error is statistical, while the second is our crude estimate of combined systematic uncertainty. It is interesting to see whether the values of f_D and f_{D_s} coming soon from the high-statistics charm program of CLEO-c would agree with our values determined by lattice QCD with exact chiral symmetry. Further, we note that in a recent 3-flavor unquenched

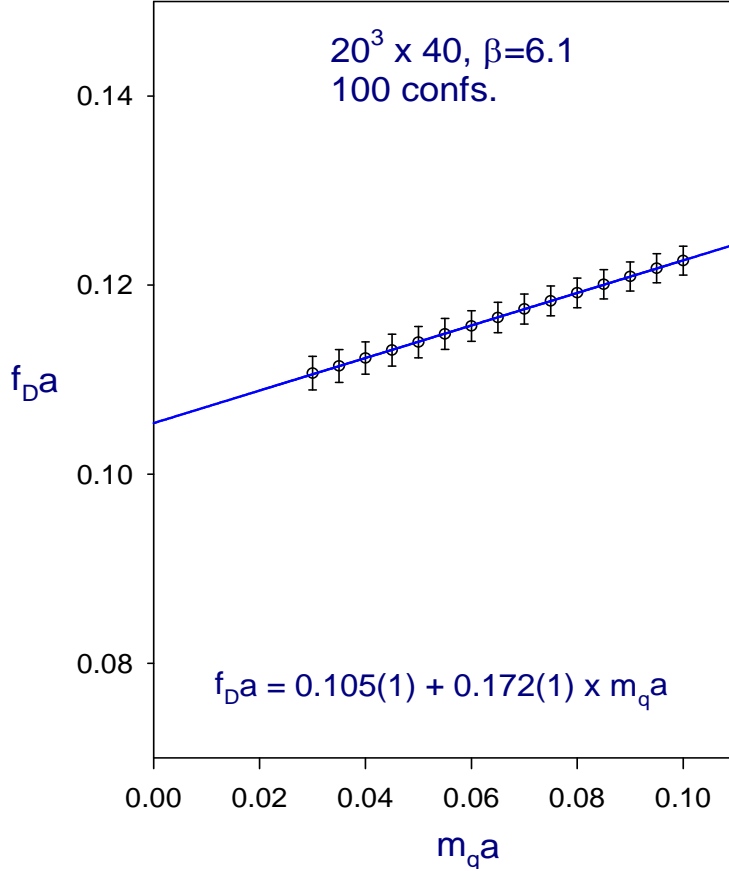


Figure 6: The D-meson decay constants $f_D a$ versus the bare quark mass $m_q a$. The solid line is the linear fit.

lattice QCD study [20] with $O(a^2)$ improved staggered light quarks and $O(a)$ -improved charm quark, their results of f_D and f_{D_s} agree with our values.

Obviously, our next task is to determinate f_B and f_{B_s} which are of fundamental importance, in view of their experimental determinations are still lacking. Since we will not use any approximations for the heavy b quark, our lattice spacing must be small enough such that $m_b a < 1$. Even though this does not seem to be formidable for f_{B_s} , it is unclear whether we can determine f_B reliably via chiral extrapolation. Presumably, f_B would behave like a function linear in m_q for a wide range of m_q , similar to f_D (Fig 6) and f_K (Fig. 4), then one should be able to obtain a reliable chiral extrapolation even for data points with $m_q > m_s$.

Acknowledgement

This work was supported in part by the National Science Council, Republic of China, under the Grant No. NSC93-2112-M002-016, and by National Center for High Performance Computation at Hsinchu. T.W.C. would like to thank Andreas Kronfeld for a timely remark at the International Conference on QCD and Hadron Physics, Beijing, June 16-20, 2005.

References

- [1] G. Bonvicini *et al.* [CLEO Collaboration], Phys. Rev. D **70**, 112004 (2004)
- [2] M. Ablikim *et al.* [BES Collaboration], Phys. Lett. B **610**, 183 (2005)
- [3] J. Z. Bai *et al.* [BES Collaboration], Phys. Rev. Lett. **74**, 4599 (1995).
- [4] K. Kodama *et al.* [Fermilab E653 Collaboration], Phys. Lett. B **382**, 299 (1996)
- [5] S. Eidelman *et al.* [Particle Data Group Collaboration], Phys. Lett. B **592**, 1 (2004).
- [6] D. B. Kaplan, Phys. Lett. B **288**, 342 (1992); Nucl. Phys. Proc. Suppl. **30**, 597 (1993).
- [7] R. Narayanan and H. Neuberger, Nucl. Phys. B **443**, 305 (1995)
- [8] H. Neuberger, Phys. Lett. B **417**, 141 (1998)
- [9] P. H. Ginsparg and K. G. Wilson, Phys. Rev. D **25**, 2649 (1982)
- [10] T. W. Chiu, Phys. Rev. Lett. **90**, 071601 (2003)
- [11] T. W. Chiu, Phys. Lett. B **552**, 97 (2003)
- [12] T. W. Chiu, hep-lat/0303008; Nucl. Phys. Proc. Suppl. **129**, 135 (2004).
- [13] N. I. Akhiezer, *Theory of approximation* (Dover, New York, 1992); *Elements of the theory of elliptic functions*, Translations of Mathematical Monographs, 79, (American Mathematical Society, Providence, RI. 1990).
- [14] H. Neuberger, Phys. Rev. Lett. **81**, 4060 (1998)
- [15] T. W. Chiu, T. H. Hsieh, C. H. Huang and T. R. Huang, Int. J. Mod. Phys. C **14**, 723 (2003)
- [16] H. Neuberger, Int. J. Mod. Phys. C **10**, 1051 (1999)
- [17] T. W. Chiu and T. H. Hsieh, Phys. Rev. E **68**, 066704 (2003)
- [18] T. W. Chiu and T. H. Hsieh, Phys. Rev. D **66**, 014506 (2002)
- [19] S. R. Sharpe, Phys. Rev. D **46**, 3146 (1992)
- [20] J. N. Simone *et al.* [The Fermilab Lattice, MILC and HPQCD Collaborations], Nucl. Phys. Proc. Suppl. **140**, 443 (2005)